

Nonparametric determination of the equation of state of Dark Energy

Houri Ziaeepour
Mullard Space Science Laboratory,
Holmbury St. Mary, Dorking, Surrey RH5 6NT, UK.
Email: hz@mssl.ucl.ac.uk

Abstract

We present a nonparametric method to determine the sign of $w + 1$ in the equation of state of dark energy. It is more tolerant to uncertainties of other cosmological parameters than fitting methods, and permits to distinguish between different classes of dark energy models even with relatively low resolution data. We apply this method to SNLS supernovae and to gold sample of re-analyzed supernovae data from Riess *et al.* 2004 [1]. Both data sets show strong indication of $w < -1$. If this result is confirmed by more extended and precise data available in near future, many of dark energy models, including simple cosmological constant, standard quintessence models without interaction between quintessence scalar field(s) and matter, and scaling models are ruled out.

Recent observations of SuperNovae (SN), Cosmic Microwave Background (CMB), and Large Scale Structures (LSS) indicate that the dominant content of the Universe is a mysterious energy with an equation of state very close to Einstein Cosmological Constant. The equation of state is defined by w , the ratio of pressure p to density ρ , $w = P/\rho$. For a cosmological constant $w = -1$. The observed mean value of w for dark energy is very close to -1 . Some of the most recent estimations are the followings: From combination of 3-year WMAP and SuperNova Legacy Survey (SNLS), $w = -0.97_{-0.09}^{+0.07}$ [2]; from combination of 3-year WMAP, large scale structure and supernova data, $w = -1.06_{-0.009}^{+0.016}$ [2]; from combination of CMAGIC supernovae analysis and baryon acoustic peak in SDSS galaxy clustering statistics at $z = 0.35$, $w = -1.21_{-0.12}^{+0.15}$ [3]; and from baryon acoustic peak alone $w = -0.8 \pm 0.18$. It is evident that with inclusion of one or two sigma uncertainty to measured mean values, the range of possible values for w runs across the critical value of -1 . Moreover, in all these measurements the value of w depends on other cosmological parameters and on their uncertainties in a complex way.

On the other hand, the sign of $\gamma \equiv w + 1$ is more crucial for distinguishing between various dark energy models than its exact value. For instance if $\gamma < 0$, scalar field (quintessence) models with conventional kinetic energy and potential are ruled out because in these models γ is always positive. Decay of dark matter to dark energy [6] [7] or in general an interaction between these components can lead to an effective $\gamma < 0$ without violating null energy condition [8] [9].

Here we propose a nonparametric method specially suitable for estimating the sign of γ . When the quality of data is adequate, it can also be used to fit the data and to measure the value of γ .

The density of the Universe at redshift z is:

$$\frac{\rho(z)}{\rho_0} = \Omega_m(1+z)^3 + \Omega_h(1+z)^4 + \Omega_{de}(1+z)^{3\gamma} \quad (1)$$

where $\rho(z)$ and ρ_0 are total density at redshift z and in local Universe, respectively; Ω_m , Ω_h , and Ω_{de} are respectively cold and hot matter, and dark energy fraction in the total density at $z = 0$. We consider a flat universe in accordance with recent observations [2]. At low redshifts, the contribution of CMB to the total mass of the Universe is negligible. The contribution of neutrinos is $\Omega_\nu h^2 = \sum m_\nu / 92.8 \text{ eV}$, $h \equiv H_0 / 100 \text{ km Mpc}^{-1} \text{ sec}^{-1}$, where H_0 is present Hubble constant. The upper limit on the sum of masses of neutrinos from 3-year WMAP is $\sum m_\nu < 0.62$ (95% confidence level) [10]. Therefore, for $z < 1$ their contribution to the total mass of the Universe is $\lesssim 4\%$ even if one of the neutrinos has

very small mass and behaves as a warm dark matter. This is less than the uncertainty on the fraction of dark matter, and thus the approximation $\Omega_m + \Omega_{de} \approx 1$ is justified. It can be easily shown that in this case:

$$\mathcal{A}(z) \equiv \frac{1}{3(1+z)^2 \rho_0} \frac{d\rho}{dz} - \Omega_m = \gamma \Omega_{de} (1+z)^{3(\gamma-1)} \quad (2)$$

Similar expressions can be obtained for non-standard cosmologies such as DGP [11] model and other string/brane inspired cosmologies [12]. It is also possible to find an expression similar to (2) for non-flat FLRW models and without neglecting hot matter. The left hand side would however depend on Ω_k , and Ω_h and would be more complex. Nonetheless, when the contribution of these components at low redshifts are much smaller than cold matter and dark energy, the general behaviour of $\mathcal{A}(z)$ will be the same as approximate case studies here.

The right hand side of (2) has the same sign as γ . Moreover, the sign of its derivative is opposite to the sign of γ because due to the smallness of observed γ , the term $\gamma - 1$ is negative. This means that \mathcal{A} is a concave or convex function of redshift, respectively for positive or negative γ , see figure 1. In the case of a cosmological constant $\mathcal{A} = 0$ for all redshifts. This second feature of expression (2) is interesting because if Ω_m is not correctly estimated, \mathcal{A} will be shifted by a constant, but this will not modify geometrical properties of $\mathcal{A}(z)$.

The left side of expression (2) can be directly estimated from observations. More specifically, Ω_m is determined from conjunction of CMB, LSS, and supernova type Ia data, and at present it is believed to be known with a precision of $\sim 5\%$. At low redshifts, the derivative of the density is best estimated from SN type Ia observations. In the case of FLRW cosmologies, the density and its derivative can be related to luminosity distance D_l , and its first and second derivatives:

$$\mathcal{A}(z) \equiv \frac{1}{3(1+z)^2 \rho_0} \frac{d\rho}{dz} = \frac{\frac{2}{1+z} \left(\frac{dD_l}{dz} - \frac{D_l}{1+z} \right) - \frac{d^2 D_l}{dz^2}}{\frac{3}{2} \left(\frac{dD_l}{dz} - \frac{D_l}{1+z} \right)^3} \quad (3)$$

$$D_l = (1+z)H_0 \int_0^z \frac{dz}{H(z)} \quad , \quad H^2(z) = \frac{8\pi G}{3} \rho(z) \quad (4)$$

It is remarkable that the right hand side of (3) depends only on one cosmological parameter, H_0 . D_l can be directly obtained from observed luminosity of standard candles such as supernovae type Ia. If only the evolution of density ρ with redshift is available, the effect of other cosmological parameters and their degeneracies are hidden in ρ and its uncertainty.

Numerical calculation of derivatives in (3) is not nontrivial. To reduce the effect of random variation of the data, it must have high resolution and low scatter, and smoothing is also necessary. The details of numerical methods applied to simulated and real data in this work is discussed in the Appendix.

We have used the data from Supernova Legacy Survey (SNLS) [4] and from low redshift supernovae ($z < 0.45$) of gold sample of re-analyzed supernovae data by Riess *et al.* 2004 [1], to estimate the sign of γ . The reason for using only the low redshift subset of supernovae from the latter compilation is that the scatter and uncertainty of the peak magnitude at higher redshifts is too large. With numerical methods used for this work, it is not possible to recover a reasonably smooth distribution for $\mathcal{A}(z)$ for comparing with models.

Fig.2 shows $\mathcal{A}(z)$ obtained from these data. To estimate the effect of the reconstruction, we compare $\mathcal{A}(z)$ from data with simulated data as described in the caption of Fig.2. In addition, we only use simulated standard sources at the same redshifts as in the data sets to make simulated samples as similar to data as possible.

We find that both data sets are closer to simulated data with $\gamma \lesssim 0$ or equivalently $w \lesssim -1$. The SNLS data is consistent with a γ as small as ~ -0.2 . There are however significant deviations from a smooth distribution for $z \lesssim 0.1$ and $z \gtrsim 0.5$. Rather considering them as genuine, we attribute them to relatively large scatter of the data at these redshifts, see Fig.3-a. To see whether the large negative γ concluded from the SNLS data is due to the data scattering and/or reconstruction algorithm artifacts,

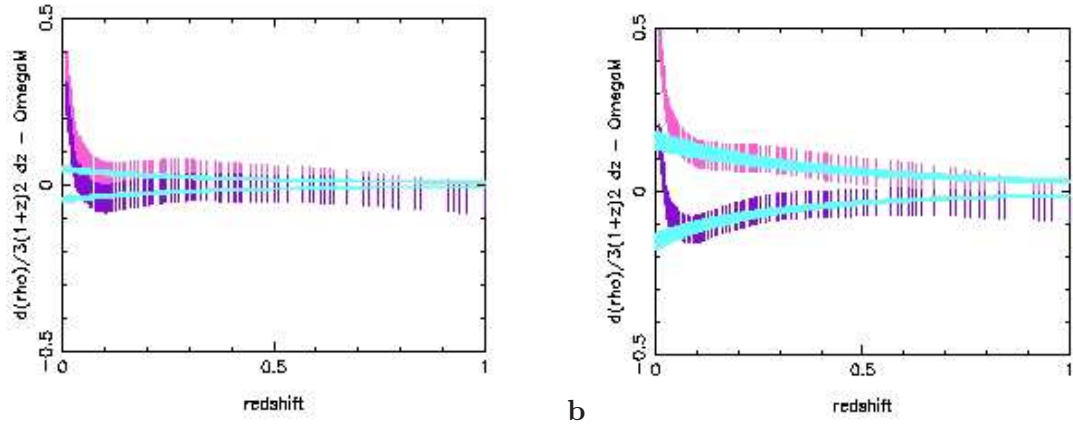


Figure 1: $\mathcal{A}(z)$ in Eq.(2) as a function of redshift; **a**: $\gamma = \pm 0.06$ (corresponding to best fit of 3-year WMAP, LSS, and SN data [2]) and **b**: $\gamma = \pm 0.2$ (corresponding to best fit of 3-year WMAP and CMAGIC SN data [3]). For both plots $H_0 = 73 \text{ km Mpc}^{-1} \text{ sec}^{-1}$ and $\Omega_{de} = 0.77$. We consider 5% of uncertainty for both quantities. Blue curves present right hand side of (2), including the uncertainty on the value of Ω_{de} . Curves decreasing or increasing with increasing redshift present respectively positive and negative γ . Magenta and purple curves present numerical determination of $\mathcal{A}(z)$ respectively for positive and negative γ from 300 simulated supernovae distributed uniformly with respect to $\log(z)$. To simulate non-uniformity of redshift distribution in observations, we randomly remove some of the simulated supernovae with equal probability for each one to be kept or removed from the set used to determine $\mathcal{A}(z)$. These plots show that numerical errors dominate near two boundaries of the redshift range. It is also evident that with this method one can distinguish between positive and negative γ for $|\gamma| \gtrsim 0.06$.

we also apply the same formalism to a subset of these data with $z < 0.45$. The result is shown in Fig.3-**b** along with simulations in the same redshift range. The *bump* at very low redshift in Fig.2 does not exist in this plot, and therefore we conclude that it is an artifact of numerical calculation. Although $\mathcal{A}(z)$ distribution in this data set is also convex - signature of $\gamma < 0$ - it does not have the same slope as any of models. More specifically, it seems that low and high redshift sections of the curve correspond to different values of γ . For $z \lesssim 0.15$, $\mathcal{A}(z)$ is close to theoretical and simulated data with $\gamma = -0.2$. For $z \gtrsim 0.25$, $\mathcal{A}(z)$ approaches the values for larger and even positive γ . Such behaviour does not appear in Fig.2. Giving the fact that the number of available data points with $z \gtrsim 0.25$ in this subset is small the most plausible explanation is simply numerical artifacts. Alternative explanations are evolution of γ with redshift and an under-estimation of Ω_m , see Eq.(2). If the latter case is true, the value of γ must be even smaller than -0.2 . With a data gap in $0.15 \lesssim z \lesssim 0.25$ interval and a small total number of entries in this data set- only 58 supernovae - it is not possible to make any definite conclusion about the behaviour of this data. We should also mention that SNLS supernovae at nearby $z < 0.25$, intermediate $0.25 < z < 0.4$, and high $z > 0.4$ redshifts are not completely treated in the same way [4]. It is therefore possible that some of the observed features explained here are purely artifacts of the analysis of raw observations.

Fig.2-**b** shows $\mathcal{A}(z)$ determined from gold sample supernovae recompiled by Riess, *et al.* [1]. Down to redshifts as low as $z \sim 0.06$ this data set is consistent with $\gamma \sim -0.06$. Although according to this plot the data is closer to the simulation with this negative γ , it is yet in 2-sigma uncertainty range of the cosmological constant model, and therefore the latter case is not completely ruled out. A positive $\gamma \gtrsim 0.06$ is much further from data and is ruled out, or at most much less plausible. As mentioned above, at higher redshifts the scatter in this data set is too large and the algorithm used here for data smoothing is not adequate.

It is not clear why the estimated values for γ from SNLS and Riess, *et al.* compilations are so different. It is most probably related to the difference in the scatter and uncertainty of these data. It is also

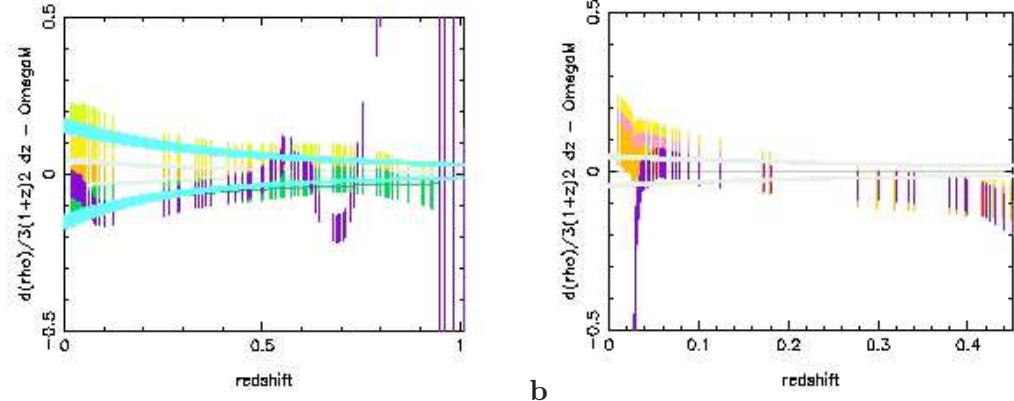


Figure 2: $\mathcal{A}(z)$ from: 117 supernovae of the SNLS data (a-purple curve), and 88 supernovae with $z < 0.45$ recompiled and re-analyzed by Riess *et al.* 2004 [1] (b-purple curve). Error bars present 1-sigma uncertainty. In (a), green, orange, yellow, and light green curves present the reconstruction of $\mathcal{A}(z)$ from simulated for $\gamma = -0.2, -0.06, 0.6, 0.2$, respectively. The same reconstruction algorithm is applied to the data and to the simulated supernovae. Light grey and cyan curves are theoretical calculation including the uncertainty on Ω_{de} , respectively for $\gamma = \pm 0.06, \pm 0.2$. In (b), the pink curve presents simulated distribution for $\gamma = 0$ - a cosmological constant. The dark grey straight line is the theoretical expectation for $\mathcal{A}(z)$ when dark energy is a cosmological constant. Definition of other curves are the same as (a).

possible that there is a systematic bias in one the data sets. It is not however trivial to quantify it and conclude which of these values for γ is a better measurement without going to the details of observations and data analysis. These issues are out of the scope of the present work. We should also mention that recent claims about contamination of supernova type Ic and the effect of asymmetric explosion in the lightcurve of supernova type Ia [13], and possible differences between low and high redshift supernovae [14] can not explain the difference between the results of these data sets. These phenomena affect both data sets in the same way. Despite these discrepancies and uncertainties, the result of both data is in good agreement with a negative γ , up to our knowledge about the physics of supernovae.

The results of present study show various shortcomings in both data sets used here. Our first remark is the large gap in redshift distribution of observed supernovae in redshift range $0.1 \lesssim z \lesssim 0.3$. Both data sets have less than 6 supernovae in this range and nothing in $0.15 \lesssim z \lesssim 0.25$. This is not an important issue for finding redshift distribution of D_l , as in all models it is a smooth function. A redshift gap becomes however very important when the purpose is the calculation of derivatives of D_l . It is possible that the lack or rareness of supernovae in this redshift range be related to the history of star formation in galaxies, and thereby to a reduced volume density of supernova explosions at these redshifts. A systematic survey of galaxies in this range is therefore necessary to increase the probability of finding supernovae and filling the present gap. Our second observation is a larger scatter in both data sets around redshift ~ 0.55 , see Fig.3-a. This leads to a large scatter in the numerical determination of derivatives in (3) and makes the results unusable, see Fig.2-a. In future observations the reason of this large scatter should be understood, and if possible reduced. From theoretical calculation and simulations shown in Fig.2 one can also conclude that with present uncertainties of cosmological parameters, the most important redshift range for determining the equation of state of dark energy is $z \lesssim 0.8$. Although the technical challenge, understanding of physics of supernovae [14] and their evolution, and applications for other astronomical ends make the findings of supernovae at larger distances interesting, they will not be in much use for determining the equation of state of dark energy, at least not at lowest level which is the determination of redshift independent component of w . These remarks are important for improvement and optimization of present and future dark energy projects.

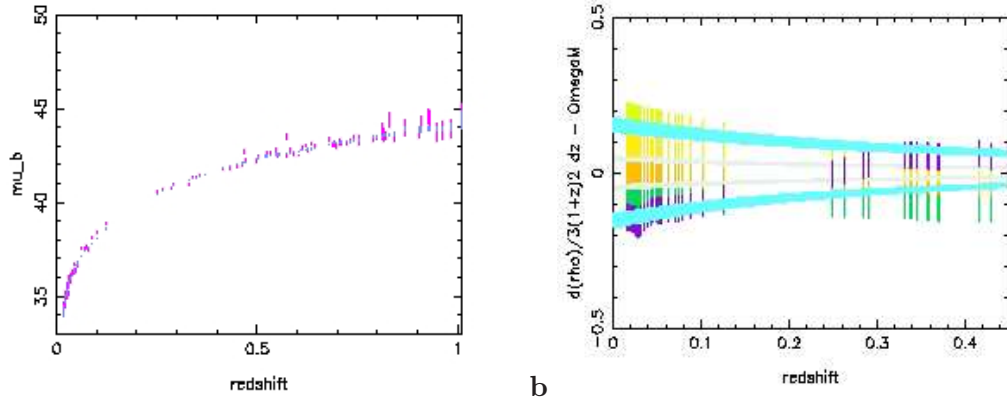


Figure 3: **a:** μ_b distribution of SNLS supernovae, data (magenta), smoothed distribution by the method explained in the Appendix (blue). Although this distribution look quite smooth, even small sudden variations can lead to large variations in derivatives. **b:** $\mathcal{A}(z)$ for SNLS supernovae with $z < 0.45$. definition of curves is the as in Fig.2.

On the other hand, improvements in numerical techniques and algorithms would also lead to better measurements. One of the possibilities in this direction is the application of an adaptive smoothing algorithm with variable degrees of smoothing depending on the amount of scattering in the data. We postpone this to future, when a larger data set becomes available.

In summary, we have proposed a nonparametric formalism to investigate the cosmological evolution of dark energy. The adventage of this method with respect to fitting is that the dependence on other cosmological parameters is explicit, and therefore it is easier to assess the effect of their uncertainties on the measurements. This method is specially suitable for applying to supernova data where the standard observable - the peak magnitude - can be directly related to cosmological distance, and thereby to cosmological variation of total density. It can also be applied to data from galaxy clustering surveys which permit to determine the variation of average density of the Universe with redshift, but not to integrated observables such as CMB anisotropy. By applying this formalism to two of largest publicly available supernovae data sets we showed that they are consistent with a $w < -1$. In one of these data sets a cosmological constant with $w = -1$ is yet possible but less favorite than $w < -1$. Present data is not however enough precise to permit the estimation of $|w|$ with good certainty. With this method and a less scattered data set, without large gaps in the redshift distribution, it would be possible to distinguish between a cosmological constant and models with w slightly deviated from the critical value of -1 . With on-going projects such as SNLS and Supernova Cosmology Project [15], and future projects such as SNAP, an enough precise data set should be available in the near future.

Appendix: Luminosity distance is related to the magnitude of an standard candle: $D_l/D_0 = 10^{\mu_b/5}$, where D_0 is the distance for which the common luminosity of standard sources is determined from theoretical models or observations. The standard magnitude at a given distance depends on H_0 and a correction must be added if a different H_0 is used in the calculation of μ_b [4].

Expression (3) for $\mathcal{A}(z)$ which is proportional to γ contains also derivatives of D_l which must be calculated numerically from data. It is however well known that direct determination of derivatives leads to large and unacceptable deviation from exact values. One of the most popular alternative methods to the direct calculation is fitting of a polynomial around each data point and then calculating an analytical derivative using the polynomial approximation in place of the data. We use this approach to determine derivatives of μ_b and D_l . In addition, before applying this approach, we smooth the distribution of magnitudes using again the same polynomial fitting algorithm.

In FLRW cosmologies the redshift evolution of the luminosity distance is very smooth. Therefore, a second order polynomial for smoothing is adequate. Fitting is based on a right-left symmetric, least χ^2 algorithm, and we have implemented *lfit* function of Numerical Recipes [16] for this purose. By

trial and error we find that 19 data-point fitting gives the most optimal results regarding the number of available data points and their scatter. The same procedure is also applied to simulated data. In present work no adaptive smoothing is applied.

References

- [1] A.G. Riess, *et al.*, *ApJ.* **607**, 2004 665, astro-ph/0402512.
- [2] D.N. Spergel, *et al.*, astro-ph/0603449.
- [3] A. Conley, *et al.*, *ApJ.* **644**, 2006 1, astro-ph/0602411.
- [4] P. Astier, *et al.*, *A&A* **447**, 2006 31, astro-ph/0510447.
- [5] D.J. Eisenstein, *et al.*, *ApJ.* **633**, 2005 560, astro-ph/0501171.
- [6] H. Ziaeepour, astro-ph/0002400.
- [7] H. Ziaeepour, *Phys. Rev. D* **69**, 2004 063512, astro-ph/0308515.
- [8] S. Das, P.S. Corasaniti, J. Khoury, *Phys. Rev. D* **73**, 2006 083509, astro-ph/0510628.
- [9] H. Ziaeepour, hep-ph/0603125.
- [10] S. Hannestad, G.G. Raffelt, astro-ph/0607101.
- [11] G. Dvali, G. Gabadadze & M. Porrati, *Phys. Lett. B* **484**, 2000 112 hep-th/0002190, *Phys. Lett. B* **484**, 2000 129 hep-th/0003054, *Phys. Lett. B* **485**, 2000 208.
- [12] P. Kanti, K.A. Olive & M. Pospelov, *PRD* **62**, 2000 126004, hep-ph/0005146, P. Binéfur, C. Deffayet & D. Langlois, *Nucl. Phys. B* **565**, 2000 269, hep-th/9905012, P. Kanti, I.I., Kogan I.I., K.A. Olive & M. Pospelov, *Phys. Lett. B* **468**, 1999 31, hep-ph/9909481, *Phys. Rev. D* **61**, 2000 106004, hep-ph/9912266; C. Csaki *et al.*, *Phys. Rev. D* **62**, 045015 2000, hep-ph/9911406, H. Ziaeepour, hep-ph/0010180 (examples of early works); V. Sahni, astro-ph/0502032 (review).
- [13] J. Middleditch, astro-ph/0608386.
- [14] A.G. Riess, M. Livio, astro-ph/0601319.
- [15] A.R. Knop *et al.*, *ApJ.* **598**, 2003 102, astro-ph/0309368.
- [16] W.H. Press, *et al.*, “Numerical Recipes in C”, Cambridge University Press.